Chapter 16 – Motors

A current challenge for the synthetic nanotechnology industry is how to transport chemical cargoes at the molecular scale in order to construct new materials, remove waste products and catalyse reactions. Nature has already evolved a wide range of efficient nanomotors that are used in a huge number of biological processes. Cells actively change their shape and move with respect to their environment e.g. the contraction of muscle cells in the heart, replication, transcription and translation of DNA, movement of macrophages to capture and remove hostile cells, division of cells during mitosis and the rotation of flagella to propel bacteria. As a common theme chemical energy derived from the hydrolysis of ATP (or GTP with microtubules) or stored in a proton gradient (with bacteria), is transformed into mechanical work to drive the cell's motility. There are currently thought to be five major mechanisms for molecular motility that occur naturally; *self-assembling motors*, *linear stepper motors*, *rotatory motors*, *extrusion nozzles* and *prestressed springs* (**figure 16.1**).

Adenosine triphosphate (*ATP*) is the central currency in energy transduction in biological systems and it is useful to examine the reaction of the molecules in more detail (**Chapter 1.10**). The dissociation of *ATP* into *ADP* and a free phosphate ion liberates a reasonable amount of energy (~20 *kT*) and is used to power a wide range of biochemical reactions,

$$ATP \underset{\longleftarrow}{\longrightarrow} ADP + P_i \qquad (16.1)$$

where *ATP* signifies a range of species with different degrees of ionisation e.g. $MgATP^{2-}$, ATP^{4-} etc, P_i is the free phosphate ion and *ADP* is adenosine diphosphate. The equilibrium constant (*K*) for energy transduction from *ATP* has the same units as concentration (M),

$$K = \frac{c_{ADP}c_{Pi}}{c_{ATP}} = 4.9\times10^{5}\,M \qquad (16.2)$$

The equilibrium constant depends on several factors such as the free magnesium concentration, the *pH* and the ionic strength. The value given for the equilibrium constant is for the standard conditions found in the cytoplasm of the vertebrate cell. The amount of energy liberated (ΔG) by the *ATP* reaction is given by

$$\Delta G = \Delta G_0 - kT\ln\frac{c_{ATP}}{c_{ADP}c_{Pi}} \qquad (16.3)$$

where ΔG is the standard free energy and ΔG_0=-54×10^{-21} J. Thus the free energy of the ATP hydrolysis reaction depends on both the standard free energy and the concentration of *ATP*, *ADP* and *P*. The *~20 kT* per ATP hydrolysis event quoted is therefore a useful rule of thumb, but more accurate calculations are possible if the specific conditions are known. Motor protein enzymes can thus liberate energy from *ATP* during conformational (mechanical) changes in their low Reynold's number aqueous environments.

The standard speed for many biological processes driven by simple molecular motors is on the order of 1 μms^{-1}. The actin filament speed of growth is around 10^{-2}-1 μms^{-1} and is dependent on the concentration of the actin filaments. Actin filament based cell crawling is also in the range 10^{-2}-1 μms^{-1} and this involves the processes of growth and disassembly of actin filaments at the leading edge of a lamellipodium (**Figure 16.1c**). Myosin interacts with actin at a rate of 10^{-2}-1 μms^{-1}. Striated muscle parallelizes the myosin/actin interactions and provides much larger forces than available from individual molecules, but with a similar time response to that of the individual molecules e.g. in human heart muscle. Microtubule growth and shrinkage is on the order of 0.1-0.6 μms^{-1} which is similar to the rate of motion of self-assembling actin fibres. Fast and slow axonal transport in neurons occurs at rates in the range 10^{-3}-10^{-1} μms^{-1} as the motor proteins kinesin and dynein walk towards the plus and minus ends of a microtubule, although these motor proteins can walk at rates as fast as 1-10 μms^{-1} in other cell types.

Nanomotors perform under low Reynolds number conditions (**Chapter 7**) and their small size means that thermal fluctuations have a large impact on their motion (Brownian perturbations). Thus nanomotors act as if they are swimming through syrup in a stochastic hurricane and a challenge is to build an intuitive picture of the unusual physical environment experienced by a nanomotor. Nanomotors are important in physiology for network structures and for signalling. An example is the movement of neurotransmitters around nerve cells, in which loss of the processivity of the motors can result in motor neuron disease.

16.1) Self-assembling motility – polymerisation of actin and tubulin

Both actin and microtubules together form the cytoskeleton of cells. Actins are found around the periphery of most mammalian cells whereas microtubules act as a transport network from the periphery of the cell to its centre (next to the nucleus). The polymerisation of actin and tubulin are examples of one dimensional aggregating self-assembly (**Section 6.8**). The rate of addition of subunits is found to be proportional to the concentration of free monomers in solution (c_m) and there is a rate constant of proportionality for the addition of monomers (k_{on}). The number of monomers captured per unit time (dn/dt) is proportional to the number of monomers available for capture (first order reaction kinetics, **Chapter 20**),

$$\frac{dn}{dt} = k_{on} c_m \qquad (16.4)$$

In contrast it is found that the release rate of monomers does not depend upon the free monomer concentration. k_{off} is a rate constant for subtraction of monomers that is independent of the monomer concentration (zeroth order reaction kinetics),

$$\frac{dn}{dt} = -k_{off} \qquad (16.5)$$

The total elongation rate of the filament is the sum of the processes for addition (equation (16.4)) and release (equation (16.5)) of the monomers provided a nucleation site for filament growth has been made available

$$\frac{dn}{dt} = k_{on} c_m - k_{off} \qquad (16.6)$$

The critical concentration (c_{mcrit}) for self-assembly occurs when the elongation rate (dn/dt) vanishes i.e. when dn/dt is equal to zero, and equation (16.6) then gives

$$c_{mcrit} = \frac{k_{off}}{k_{on}} \qquad (16.7)$$

Figure 16.2 shows a graphical solution of equation (16.6) for one dimensional aggregating self-assembly. Above the critical monomer concentration the fibres expand, whereas below this concentration they shrink.

Similar processes of self-assembly are observed experimentally for both actin and tubulin filaments. In principle it is easy to extract the rate constants for addition and subtraction of the monomer subunits (k_{on} and k_{off}) from in vitro experiments from a plot of the elongation rate as a function of the monomer concentration. There are however some additional complications with real self-assembling biological motors. Subunits are not symmetrical and add to each other with a preferred orientation, which gives rise to oriented filaments (**figure 16.3**). The two ends of the polymer are not chemically equivalent. The faster growing end is referred to as the plus end and the slower growing end is labelled with a minus sign. Thus experimentally the two ends (+ and -) of the self-assembling filament need to be considered separately to extract the two sets of rate constants for addition and subtraction. It is found that the rate constants depend on both the solvent and salt concentration, so the aqueous environment that surrounds the filaments needs to be carefully monitored.

This situation of anisotropic self-assembly can be analysed through an extension of the Oosawa model described by equation (16.6) (**figure 16.4** and **16.5**). Since the two ends of the filament are not equivalent two equations are needed for the rate of elongation of each of the two ends,

$$\frac{dn^+}{dt} = k_{on}^+ c_m - k_{off}^+ \qquad (16.8)$$

$$\frac{dn^-}{dt} = k_{on}^- c_m - k_{off}^- \qquad (16.9)$$

Each of these equations has a separate critical monomer concentration for the process of self-assembly ($\frac{dn^+}{dt} = 0$, $\frac{dn^-}{dt} = 0$),

$$c_{m+crit} = \frac{k_{off}^+}{k_{on}^+} \qquad (16.10)$$

$$c_{m-crit} = \frac{k_{off}^-}{k_{on}^-} \qquad (16.11)$$

In the special case that the critical concentration of both ends are equal (c_{m+crit}=c_{m-crit}) both ends grow or shrink simultaneously, although the rates of assembly may be different. For steady state conditions (tread milling) the rate of growth and shrinkage of the two ends must be equal. This can be expressed mathematically as

$$\frac{dn^+}{dt} = -\frac{dn^-}{dt} \qquad (16.12)$$

And there is therefore a single critical concentration (c_{mtm}) for this process of tread milling self-assembly,

$$c_{mtm} = \frac{\left(k_{off}^+ + k_{off}^-\right)}{k_{on}^+ + k_{on}^-} \qquad (16.13)$$

The process of tread milling is schematically shown in **figure 16.6**, the length of the filament is invariant during the process, but its centre of mass is displaced to the right. **Table 16.1** gives some typical values for the rate constants and the critical concentrations during the self-assembly of actin and microtubules. Tread milling often occurs in vivo, since it is highly efficient in the reuse of subunits.

The varieties of interactions and their pattern formation in active self-assembling motor protein networks can be very complex. An example of a dynamic morphology created during cell division is shown in **figure 16.7**. Here an animal cell is shown in the final stages of cell division (cytokinesis) where an actin/myosin ring contracts to pinch off the two divided cells. Also shown is the remains of the mitotic spindle formed from microtubules that drives the movement of the chromosome in the initial stages of cell division.

The amoeboid motility of many cells is achieved by self-assembly of actin filaments at the leading edge of the cell (**figure 16.8**). However in vivo there are a complex collection of actin associating proteins (e.g. branching or capping proteins) that direct the process of self-assembly.

16.2) Parallelised linear stepper motors – striated muscle

The basic constituents of striated muscle are actin and myosin which are arranged in a parallel array (**figure 16.9**). These motors are perhaps the most important for human health, since heart disease provides the largest contribution to annual human mortality rates and the majority of the muscle in hearts is striated.

A scheme for the chemomechanical transduction process that use *ATP* to provide motility in striated muscle is provided by the rotating cross-bridge model (**figure 16.10**). This involves two key ideas; the myosin motors cycle between attached and detached states, and the motor undergoes a conformational change (the working stroke) that moves the load bearing region of the motor in a specific direction along the filament. The rotating cross bridge model incorporates the Lymn-Taylor scheme which describes chemically how nucleotides (ATP, ADP) regulate the attachment and detachment of myosin from the filament, the swinging lever arm hypothesis which provides a mechanism for the amplification of small structural changes around the nucleotide-binding pocket into much larger conformational changes of the cross-bridge, and the power-stroke model which accounts for how the motor generates force through the use of an elastic element within the cross bridge that is strained during the power stroke.

During the action of striated muscle there is a sequence of transitions between different chemical states of the myosin molecules; *ATP* binding, *ATP* hydrolysis and *ADP* release. These transitions alter the association between the motor domain and the filament, which leads to the alternation between attached and detached states.

There are three distances required to understand the inch worm motion of myosin along the actin filaments. The *working distance* (δ) is the distance a cross bridge moves during the attached phase of its hydrolysis cycle. The *distance per ATP* (Δ), is the distance that each motor domain moves during the time it takes to complete a cycle, which is also equal to the speed of movement divided by the ATPase (the part of the myosin that acts as an ATP enzyme) rate per head. The *path distance* is the distance between consecutive myosin binding sites (or stepping stones) (**figure 16.11**) along the actin fibre.

A series of single molecule techniques have been used to measure the forces and characteristic distances used by myosins that associate with single fibres of actin. Force transducers that are typically used are cantilevered glass rods, atomic force microscopes (AFM) and dual-trap optical tweezers (**Section 13.4**). A particularly elegant experiment uses an actin filament attached at either end to two optically trapped spheres and the actin interacts with single myosin II molecules (**figure 16.12**). Single working strokes of the myosin molecules are resolvable with this method. Single molecule fluorescence is another powerful technique to

follow the pathway of a motor protein reaction and microrheology techniques can resolve the changes in viscoelasticity due to the motion of active molecular motors.

It is useful to consider the exact nature of the molecular steps of myosin II that travel along an actin filament. The myosin has five structural configurations during its interaction with actin in muscular motion (**figure 16.13**). Initially there is tight binding of the myosin head to the actin filament, called the rigor position (as in rigor mortis where the additional cross-links account for the rigidity of dead muscle). Next the myosin filament is released when it captures *ATP*, which provides the energy for the force on the actin fibre. There is then a configurational change to the cocked position during hydrolysis of *ATP*. Subsequently there is weak binding of the head to the myosin filament in a new position and finally a phosphate group is released.

The speed and processivity of the crossbridge motion can be understood using the concept of the duty ratio, which is the fraction of the time each motor domain spends attached to its filament. There is a cyclic process (**figure 16.14**) in which the motor repeatedly binds to and unbinds from the filament. During each cross bridge cycle, a motor domain spends an average time attached to the filament (τ_{on}) when it makes it working stroke and an average time detached from the filament (τ_{off}) when it makes its recovery stroke. The duty ratio is the fraction of time that each head spends in its attached phase,

$$r = \frac{\tau_{on}}{\tau_{on} + \tau_{off}} \qquad (16.14)$$

The minimum number of heads (N_{min}) required for continuous movement (N_{min}) is thus related to the duty ratio,

$$r \approx \frac{1}{N_{\min}} \qquad (16.15)$$

Single stepper motors are parallelized to provide much larger forces, but with a reasonably fast time response in striated muscle.

For the striated muscle in the human bicep it is possible to make a quick calculation for the force exerted by each myosin molecule. The number of myosin chains is equal to the cross-sectional area of the muscle divided by the cross-sectional area of a single thick filament multiplied by the number of myosins per thick filament,

$$N_{myosin} \approx (\textit{Cross-sectional area of muscle/Cross-sectional area of thick filament}) \times N_{myosin}\ \textit{per thick filament}$$
$$\approx \pi(3\ cm)^2/\pi(60\ cm)^2 \times 300 \approx 10^{14} \qquad (16.16)$$

A 10 kg weight can be comfortably lifted by a human bicep, so an order of magnitude estimate gives the force per myosin as

$$F_{myosin} \approx 10\ kg \times 10\ ms^{-2}/10^{14} = 1\ pN \qquad (16.17)$$

This value of the force per myson is in reasonable agreement with that measured in a single molecule experiment.

Stepper motors also occur in a wide range of roles other than in striated muscle. Inside eukaryotic cells motor proteins are required to drive the motion of vesicles. Dynein motor proteins drive cargoes towards the nucleus, whereas kinesins move vesicles to the cell periphery and myosins move cargoes around the actin cytoskeleton at the cell periphery (**figure 16.15**). For single stepper motors another simple estimate of the force exerted during a single motor step can be made. Consider a dynein molecule that moves 8 nm along a microtubule per *ATP* hydrolysis event (8 nm is the repeat distance of monomers along the microtubule). The force (F_{max}) exerted by the dynein walking on a microtubule (or kinesin using an equivalent approximation) is the energy divided by the distance moved,

$$F_{max} = \textit{free energy of ATP hydrolysis/step size} \approx 20\ kT/8\ nm \approx 10\ pN \qquad (16.18)$$

Therefore 10 pN is an upper limit on the force that dynein can exert, since it assumes that the motor is 100% efficient.

A current challenge is to understand the regulation of the different modes of transport of vesicles inside cells. Stochastic stepping motion of veiscles is observed in live cells with well regulated changes in speed and direction. How this relates to the activity of multiple motor proteins attached to a single vesicle is not well understood e.g. does a tug of war take place between opposing polarity microtubule motors (opposing teams of dynein molecules versus kinesin molecules)?

16.3) Rotatory motors

Following on from the discussion of Poisson motility processes of bacteria in **Section 7.3** the molecular biophysics of the rotatory flagellar motor for the propulsion of bacteria will be considered (**figure 16.16**). The *ATP* synthase in the mitochondria of eukaryotic cells converts *ADP* into *ATP*. It is also a rotary motor and is driven by a *pH* gradient (in common with the bacterial motor, but the process occurs in reverse, ADP→ATP for the synthase rather than ATP→ADP in the flagellar motor). Nature thus invented the wheel billions of years before man and it has a number of different roles.

A curved segment separates the motor from the main length of the filament in bacteria (**figure 16.17**). The filament is bent away perpendicularly from the surface of the membrane for several nanometres. This filament executes a helical motion as it rotated by the motor and acts like a propeller which provides a source of motility for the bacteria.

A series of proteins form the flagellum of the bacterium and each has a specific function; the bushings seal the cell membrane, the circular stator is attached to the cell and the rotor is connected to the flagellum (**figure 16.1a**). The flagellar propeller is not run directly by *ATP*. Instead protons run down a pH gradient across the membrane and produce an electric potential. Variation of the *pH* drop across a membrane can change the direction of the motor. Sodium ions also can fulfil the same function as hydrogen ions in some marine bacteria. As bacteria move through a solution their flagella can rotate at up to 100 $revs^{-1}$, which is comparable to the rate at which an automobile petrol engine (30 $revs^{-1}$) functions. The flagellar motor works equally well in both clockwise and counter clockwise modes. These bacterial motors are relatively complicated devices and consist of over twenty separate protein components that only together can provide motility. The evolutionary history of the creation of such a finely orchestrated engine is a fascinating story.

Steps in the rotatory motion of a bacterial motor can be observed by attachment of a fluorescent actin filament to the hook subunit in fluorescence microscopy experiments. Discrete quantised angular movements of the motor are observed. The rate of rotatory motion is found to be proportional to the potential difference across the motor under physiological conditions.

16.4) Ratchet models

An interesting, but inefficient (and thus inaccurate) model of molecular motility is provided by the thermal ratchet. The model demonstrates how directed motility of a muscle protein can be derived from rectified Brownian motion (**figure 16.18**) i.e. a constant probability bias is superposed on the thermal fluctuations of displacement of a particle in a particular direction. Widely differing processes of motor driven motility such as stepper motors and rotatory motors can be described in terms of rectified Brownian motion, as a unifying principle, and ratchet models have thus been widely used to analyse their motion.

The thermal ratchet is a simple mechanism to produce motion in a low Reynold's number environment. It uses a spatially asymmetric potential that oscillates with time (**figure 16.19**). The probabibity distribution of motor proteins ($P(x)$) as a function of distance (x) evolves due to diffusion in the standard Brownian fashion due to thermal motion when the potential is switched off (**Section 7.1**). The asymmetry of an oscillating saw tooth potential, when supperposed on the thermal fluctuating force, causes a net motion of the proteins in a given direction. The net probability of directed motion (P_{net}) is the difference between the probability to move right (P_R) and that to move left (P_L),

$$P_{net} = P_R - P_L \qquad (16.19)$$

A simple mathematical form for the probability distribution of the motor proteins results from the action of the saw tooth potential. If the proteins do not diffuse a sufficient distance there is no net flux,

$$P_{net} = 0 \qquad 0 < \sigma < \alpha x \qquad (16.20)$$

where x is the wavelength of the saw tooth potential, σ is a measure of the spread of the particle distribution and αx is the peak-to-trough separation of the potential. If the probability distribution created by the thermal motion is sufficiently broad, a net flux occurs,

$$P_{net} = (1 - \alpha x/\sigma)^2/2 \qquad \alpha x < \sigma < (1-\alpha)x \qquad (16.21)$$

The probability distribution initially broadens when the potential is not applied due to thermal diffusion of the motor proteins. When the potential is switched on again there is a higher probability that the particles are drawn to the right than to the left, due to the asymmetric nature of the potential. This allows the dipolar nature of the motion of the monomers along the biofilament to be modelled.

The major problem with such a simple Brownian ratchet model is its efficiency. A thermal ratchet can take the hydrolysis of up to 10 *ATP* molecules for 1 step ($P_{net}=0.1$). In real biological systems the efficiency

is typically 5 times better than that found for the model (**figure 16.8**). More sophisticated extensions of such models have recently been proposed that resolve this shortfall.

Ratchet models have also been applied to rotatory motors (**figure 16.1a**). An elastic link is invoked between the stator unit and the cell wall that rectifies the angular thermal fluctuations in a certain sense (anticlockwise or clockwise), which creates directed motion.

16.5) Other systems.

Other less common mechanisms for biological motility have been discovered. *Extrusion nozzles* are present in the myxbacteria, cyanobacteria and flexibacteria. Slow uniform gliding motion is achieved for these organisms by a continuous secretion of a glycoprotein slime (**figure 16.1d**).

Supramolecular springs store conformational energy in chemical bonds that can then act as latches for its release (**figure 16.1e**). The specific power of such motors can be very high. One example is the scruin/actin system in which scruin captures actin in a slightly over twisted state. Calcium dependent changes in the scruin are then used to release the conformational energy of the actin and provide a force for motility.

In bacteriophage the DNA is stored at very high osmotic pressures. A translocation motor is thus needed to accomplish this process of packaging when the DNA is pushed through the pore in the bacteriophage's coat proteins (**figure 16.20**). Binding of proteins inside the bacteriophage are thought to facilitate the transport of the DNA chain into the bacteriophage.

It is expected that many more nanomotor systems will continue to be discovered and the list above is by no means exhaustive e.g. gas filled bubbles in aquatic microorganisms allow them to adjust their feeding depth.

Suggested Reading

If you can only read one book then try

J.Howard, 'Mechanics of Motor Proteins and the Cytoskeleton', Sinauer, 2001. Very good introductory text on motor proteins.

D.Boal, 'Mechanics of the Cell', CUP, 2011, 2nd edition. Contains a useful section on active molecular networks.

R.Phillips, J.Londev, J.Theriot, H.Garcia, 'Physical biology of the cell', Garland, 2012. Useful description of statistical models for motor protein activity.

D.Bray, 'Cell movements: from molecules to motility', Garland, 2000. Classic text on both biological motors and microorganism motility.

S.Vogel, 'Prime mover: a natural history of muscle', W.W.Norton, 2002. Popular introduction to the biology of muscle.

P.M.Hoffmann, 'Life's ratchet', Perseus, 2012. Excellent popular account of the biophysics of nanomotors.

Tutorial questions16

16.1) Make a list of the molecular motors that occur in biology. Name some diseases associated with malfunctioning motor proteins.

16.2) Describe the factors that affect the maximum rate of the motion and the force that can be exerted by an actin filament.

16.3) Using **Table 16.1** check that the relationship between the critical monomer concentration and the dissociations constants (equations 16.10 and 16.11). Calculate the critical concentrations for tread milling of actin and microtubules.

Tables

Monomer in solution	k_{on}^{+} $(\mu Ms)^{-1}$	k_{off}^{+}, s^{-1}	k_{on}^{-} $(\mu Ms)^{-1}$	k_{off}^{-}, s^{-1}	$c_{m+crit,}$ μM	$c_{m-crit,}$ μM
Actin						
ATP-actin	11.6	1.4	1.3	0.8	0.12	0.6
ADP-actin	3.8	7.2	0.16	0.27	1.9	1.7
Microtubules						
Growing (GTP)	8.9	44	4.3	23	4.9	5.3
Rapid	0	733	0	915	N/A	N/A

disassembly						

Table 16.1. Rate constants (k_{on} for addition of a subunit and k_{off} for the dissociation of a subunit) and critical micelle concentration for actin and microtubule self-assembly at both the + and – ends of the filaments [*Ref. T.D.Pollard, J.Cell.Biol.,1986, 103, 2747-2754*].

Figures

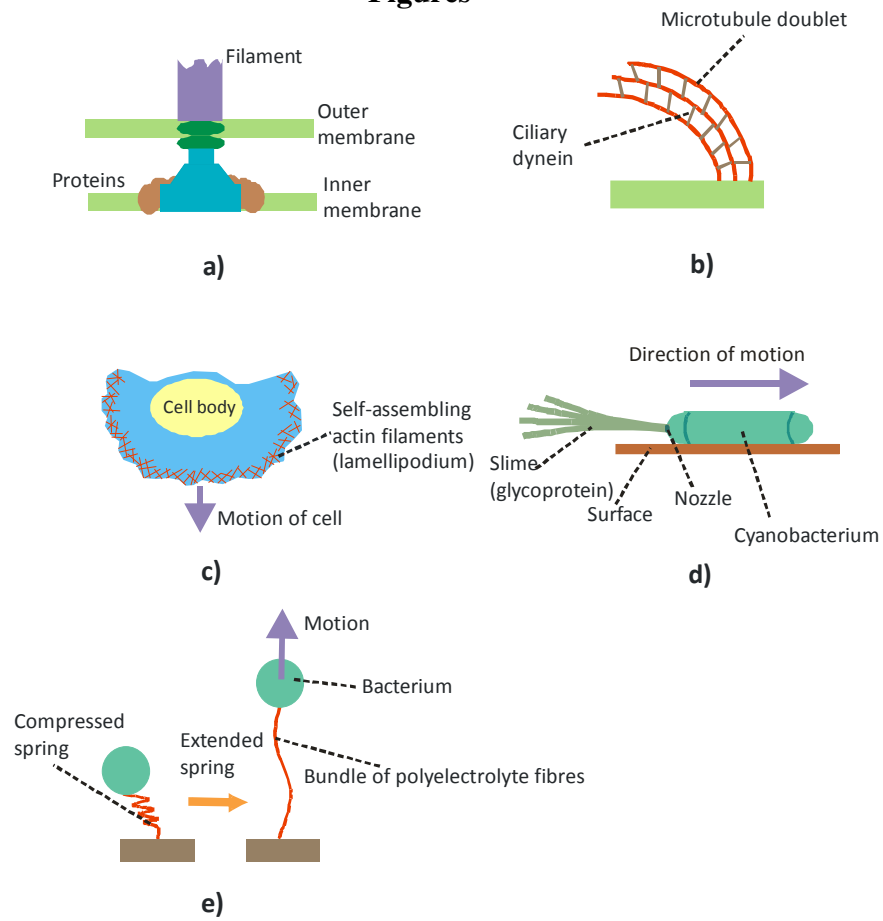

Figure 16.1. Examples of the five separate strategies for biological motors; a) *rotatory motors* in bacterial locomotion, b) *linear stepper motors* in cilia, c) *self-assembling motors* formed from actin filaments in lamellipodium, d) *extrusion nozzles* in cyanobacterium, and e) *prestressed springs* in bacterial locomotion.

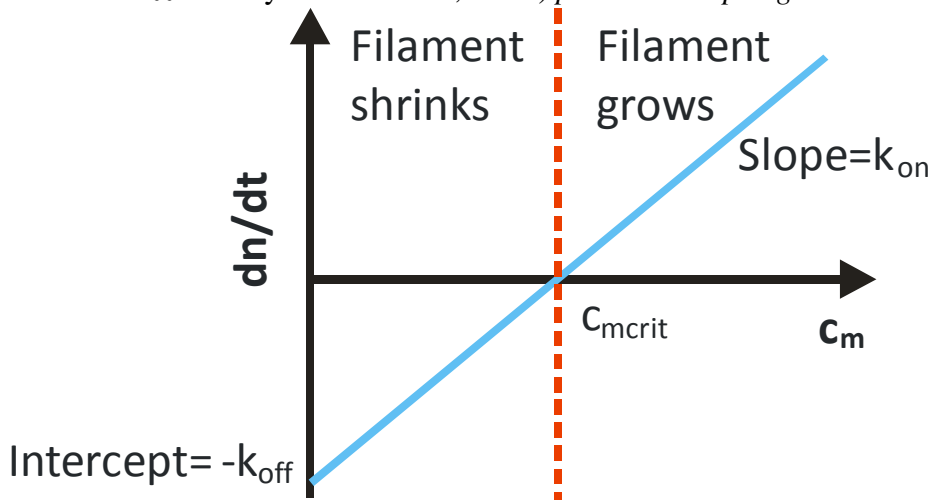

Figure 16.2. The rate of polymerisation of actin filaments (*dn/dt*) as a function of monomer concentration (c_m). c_{mcrit} is the critical monomer concentration for self-assembly. Below c_{mcrit} the filaments shrink and above c_{mcrit} they grow. The gradient of the figure gives the association rate constant (k_{on}) and the *dn/dt* intercept gives the dissociation rate constant ($-k_{off}$).

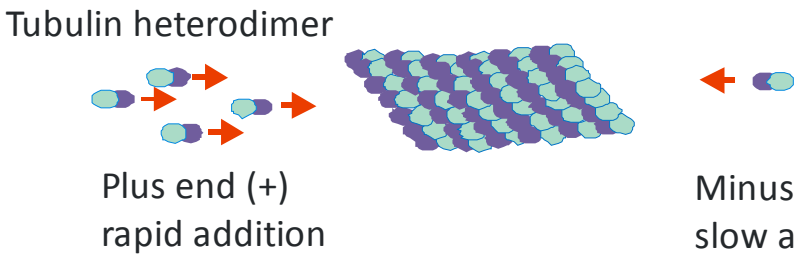

Figure 16.3. The self-assembly of tubulin (and actin) is anisotropic, due to the anisotropy of the constituent subunits. Fast addition occurs at the positive end (+) and slow addition on the negative end (-).

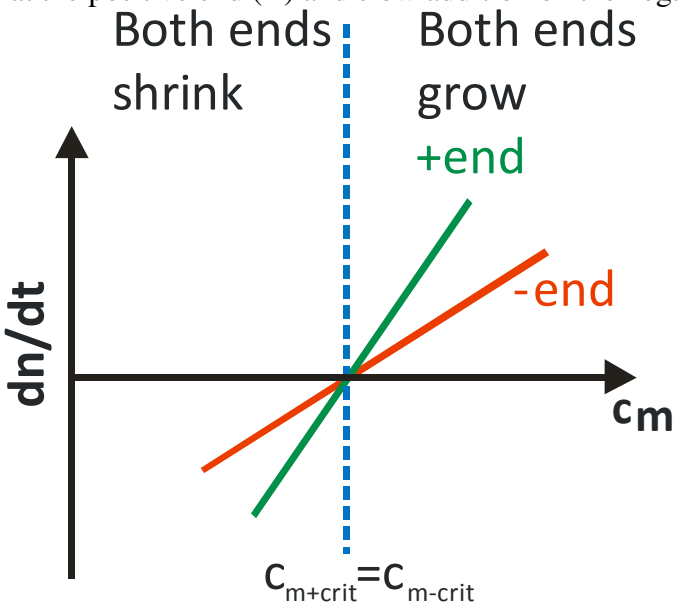

Figure 16.4. Model for the dynamics of actin self-assembly that considers the different rate constants for both ends of the anisotropic filament. The rate of assembly (*dn/dt*) is shown as a function of the monomer concentration (c_m). In the case illustrated $c_{m+crit}=c_{m-crit}$.

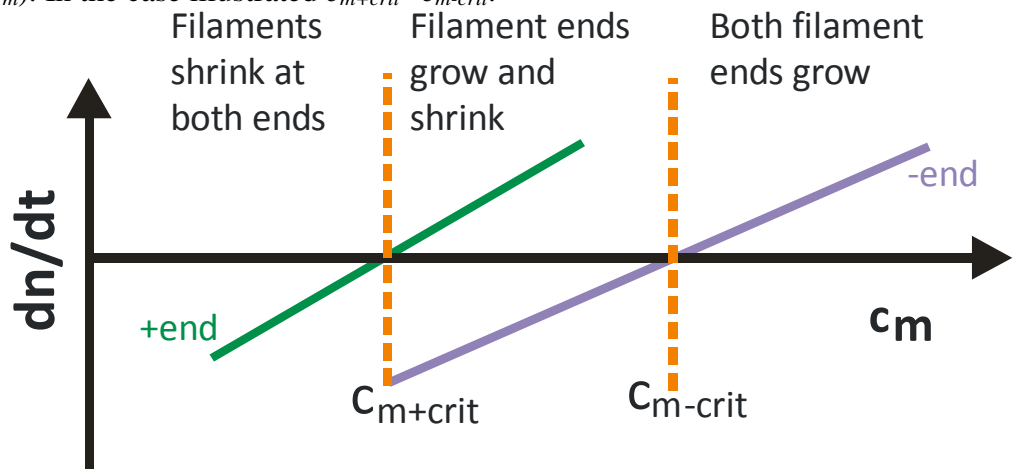

Figure 16.5. Model for the dynamics of actin self-assembly in which $c_{m+crit} \neq c_{m-crit}$ during the assembly of the anisotropic filaments. The rate of assembly (*dn/dt*) is shown as a function of the monomer concentration (c_m).

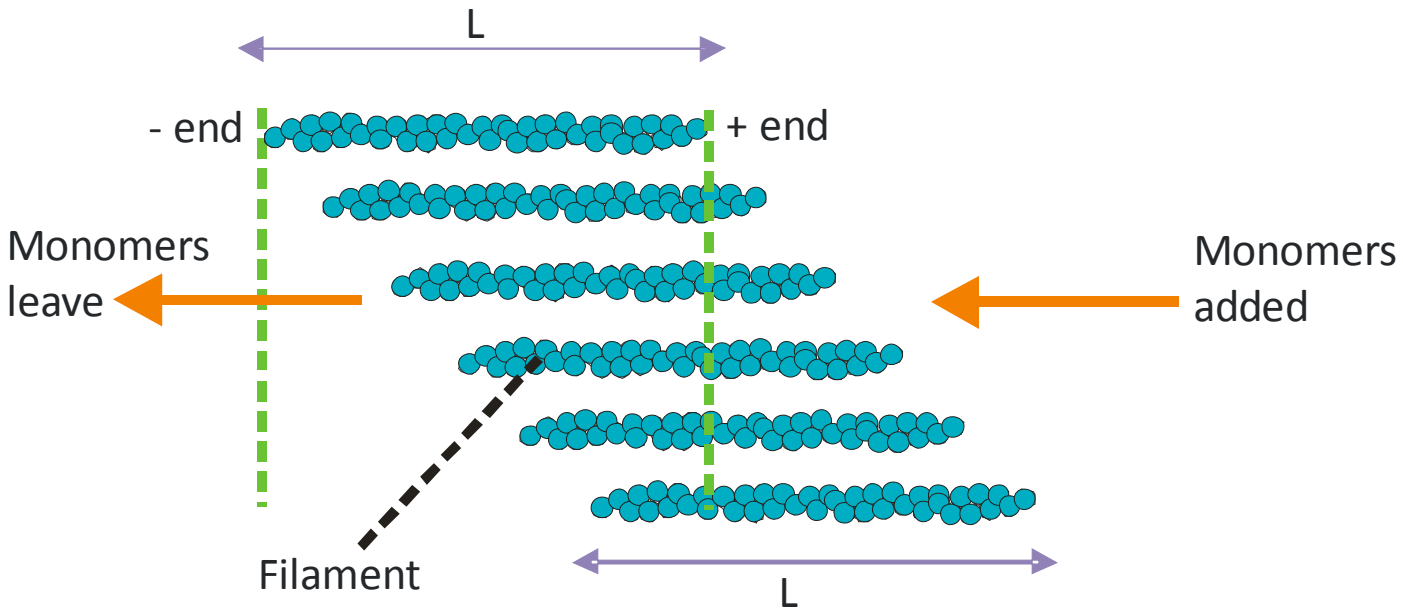

Figure 16.6. The treadmilling process involved in actin self-assembly. Monomers leave from the negative end and are added to the positive end. The filament length (L) is conserved during the process, as the centre of mass of the filament moves to the right.

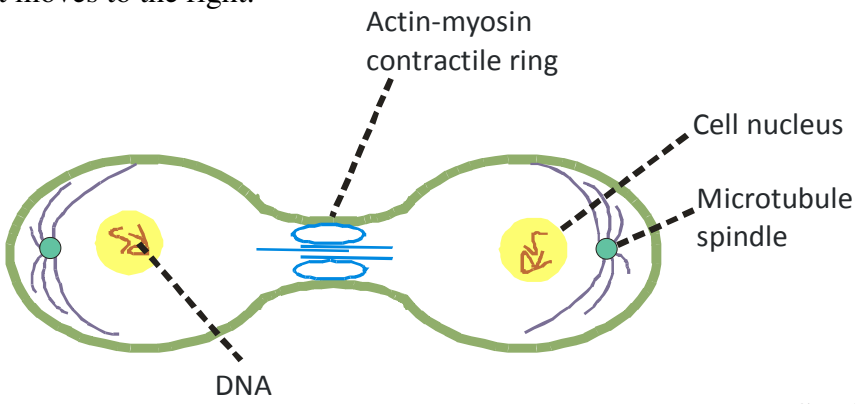

Figure 16.7. The motor proteins involved during the cytokinesis of cell division (**Section 2.9**). The actin-myosin ring pinches off the cell in the final stages of replication. The microtubule spindle is used in a prior step in the process of chromosomal division.

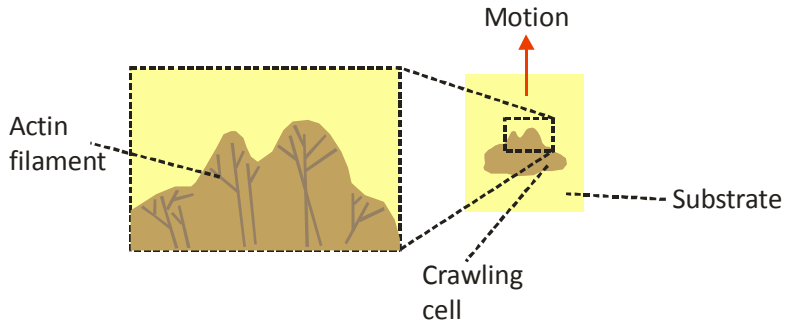

Figure 16.8. Branched self-assembly of actin filaments drives the amoeboid motion of cells in vivo.

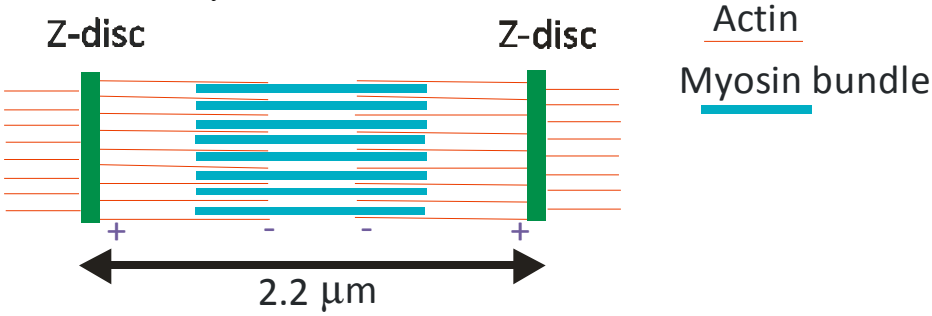

Figure 16.9. The arrangement of actin and myosin that are parallelised into arrays in striated muscle e.g. heart muscle or the muscle in a bicep. The distance between the Z-discs decreases during muscular contraction as the myosin molecules walk along the actin filaments.

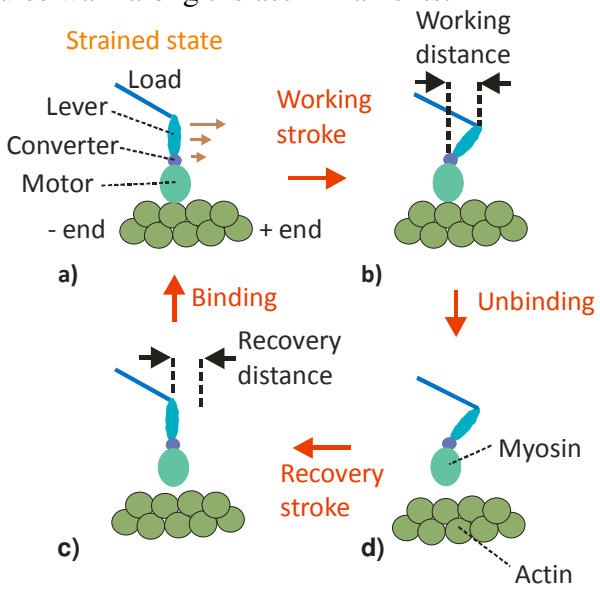

Figure 16.10. The rotating cross bridge model for myosin/actin association consists of four distinct steps. a) The myosin attaches to the actin filament, b) the myosin molecule does work as it stresses the binding site, c) the myosin unbinds from the actin filament and d) the stress in the myosin molecule is dissipated as it moves one step along the actin filament.

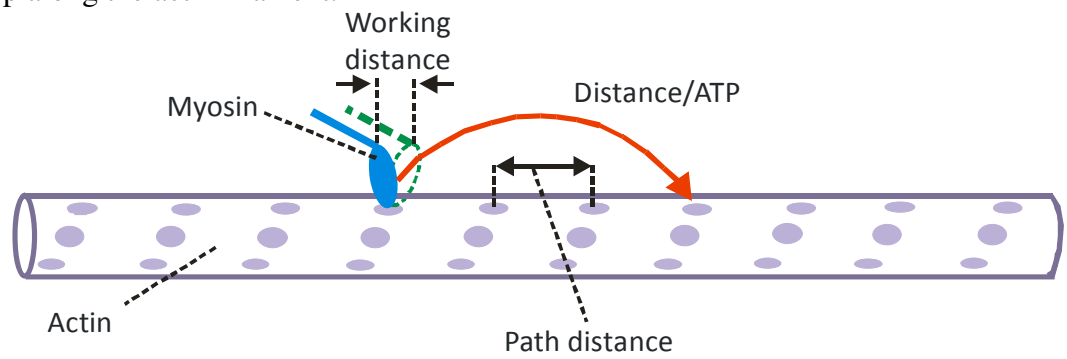

Figure 16.11. Three distances associated with the inch worm motion of myosin molecules along actin. The working distance is the length moved by a myosin molecule in each cycle of the rotating cross bridge model, the path distance is the lateral distance between binding sites and the distance per *ATP* is the length moved by a myosin molecule that uses one molecule of *ATP* [*Ref. J.Howard, Mechanics of Motor Proteins and the Cytoskeleton, Sinauer, 2001*].

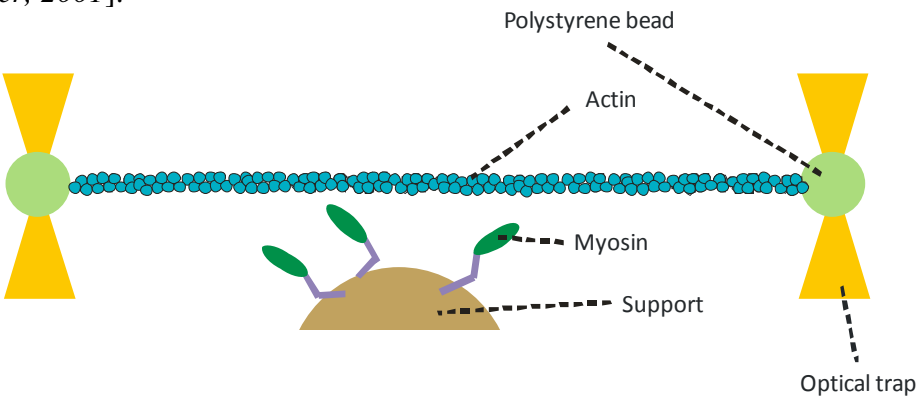

Figure 16.12. Double trap optical tweezers can be used to measure the step size of myosin II motors when they interact with actin filaments. The actin filament is attached at either end to optically trapped colloidal beads (polystyrene).

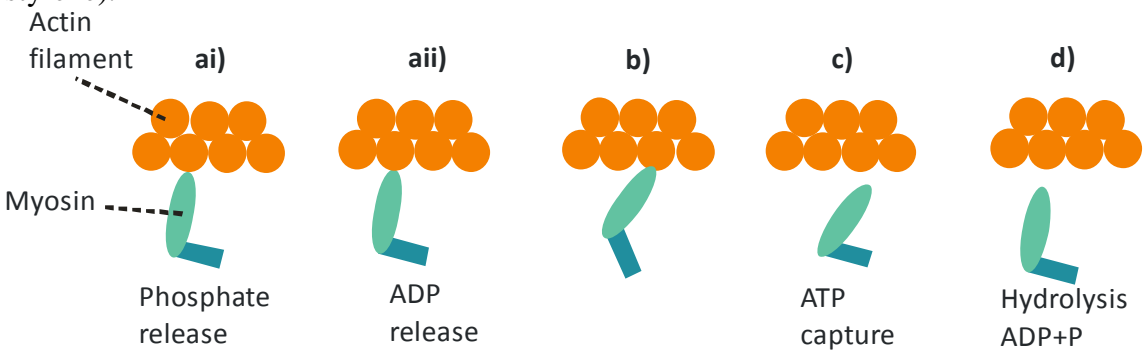

Figure 16.13. Chemical steps in the cyclic attachment of myosin to actin filaments that corresponds to the rotating cross-bridge model (**figure 16.10**).

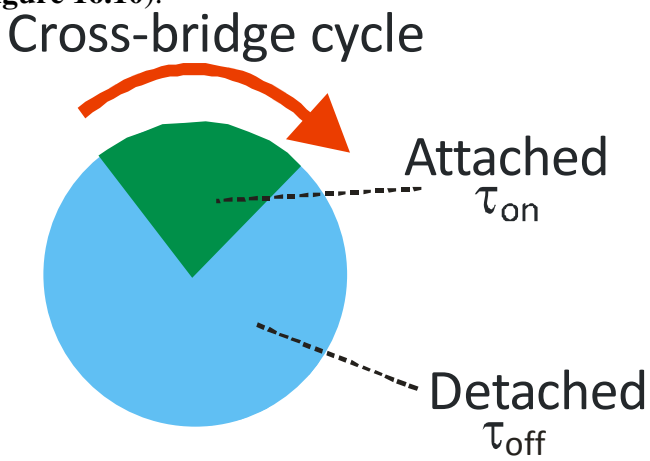

Figure 16.14. Crossbridge cycle with myosin binding to actin filaments. τ_{on} is the attached time and τ_{off} is the detached time. The cycle rotates through alternating periods of attachment and detachment.

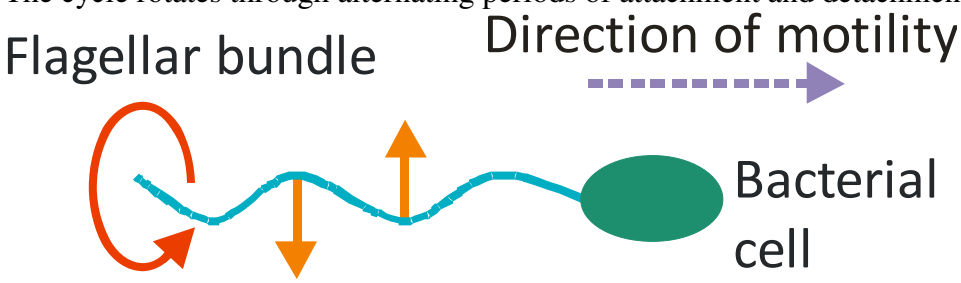

Figure 16.15. Helical flagellar filaments provide a bacterium with motility in its low Reynold's number environment. Ecoli cells typically have multiple flagellae (6) attached to their surface, so forward motility is driven by the action of a coherent bundle of flagellae.

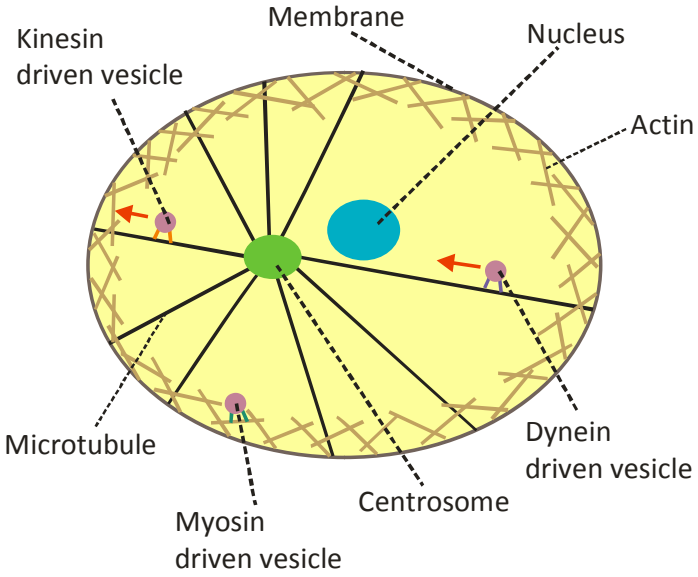

Figure 16.16. The stepper motors dynein, kinesin and myosin drive the motion of vesicles inside eukaryotic cells. Myosins travel along actins at the cell periphery. Dyneins drive transport towards the cell nucleus along microtubules and kinesins drive transport in the opposite direction.

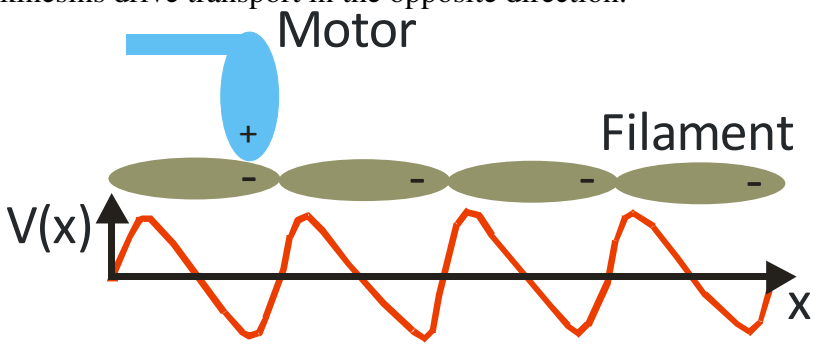

Figure 16.17. The interaction of motor proteins (e.g. myosin) with actin can be modelled with a single one dimensional potential ($V(x)$) as a function of distance (x). The monomers of a biofilament have a dipolar charge distribution and the myosin motors experience a saw tooth interaction potential ($V(x)$) as they interact with the filament.

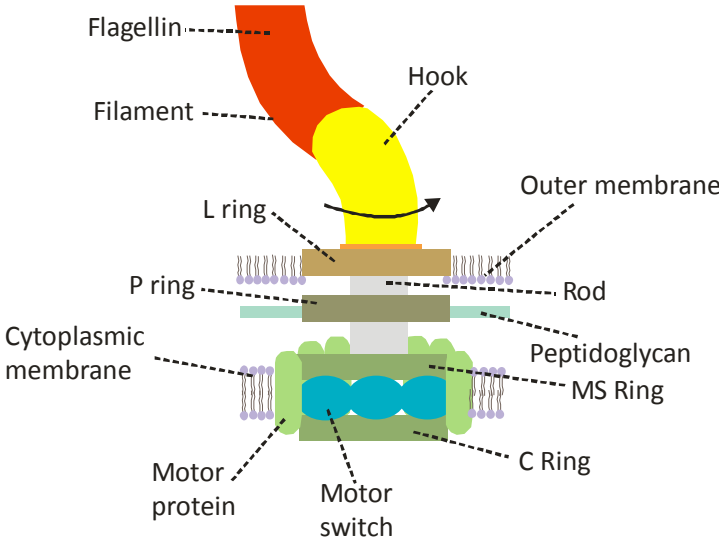

Figure 16.18. The rotatory motor attached to the flagellae of bacteria is constructed from over twenty different types of protein (also seen in **figure 16.15**). The motor is driven by a gradient of hydrogen ions.

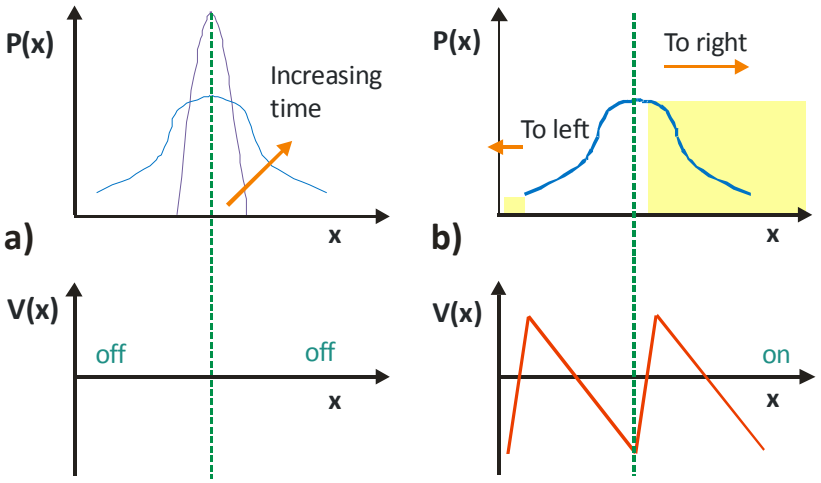

Figure 16.19. An oscillating saw tooth potential ($V(x)$) as a function of distance (x) can be used to move a series of particles (probability density $P(x)$). Within this realisation of the ratchet model particles are moved to the right by the asymmetry of the saw tooth potential. a) The particle probability distribution and potential when the ratchet is switched off. b) The particle probability distribution and potential when the ratchet is switched on [*Ref. J.Prost, J.F.Chauwin, L.Peliti, A.Ajdari, PRL, 1994, 72, 16, 2652-2655 and R.D.Astumian, M.Bier, PRL, 1994, 72, 11, 1766-1769*].

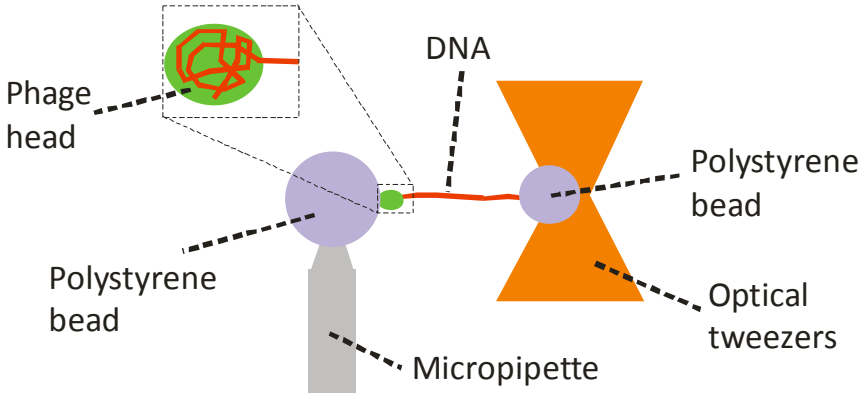

Figure 16.20. A motor on the head of a bacteriophage can be used to compact a DNA chain into the interior of the head. The forces involved can be measured using optical tweezers.